Quasiguided surface plasmon excitations in anisotropic materials

Marco Liscidini[1] and J. E. Sipe[2]
[1]*Department of Physics "A. Volta," University of Pavia, Via Bassi 6, I-27100 Pavia, Italy*
[2]*Department of Physics and Institute for Optical Sciences, University of Toronto, 60 St. George Street, Toronto, Ontario, Canada M5S 1A7*

(Received 21 December 2009; revised manuscript received 29 January 2010; published 31 March 2010)

We present a theoretical study of surface plasmon polaritons in a configuration where a metal layer is bounded by a homogeneous anisotropic dielectric. We consider uniaxial and biaxial dielectrics with the optical axis lying in the plane defined by the metal/dielectric interface. Through a systematic study of the in-plane surface plasmon dispersion relation we confirm the existence of several propagation regimes for different values and signs of the birefringence. We report the discovery of the existence of quasiguided surface plasmon polaritons characterized by non-null radiative components. We identify the conditions for the existence of such modes, and explain their peculiar properties in terms of the hybridization of radiative and guided modes.

DOI: 10.1103/PhysRevB.81.115335 PACS number(s): 78.20.Bh, 78.67.−n, 42.70.Qs

I. INTRODUCTION

Surface plasmons and related excitations have now been studied for over half a century.[1,2] Recent progress in the fabrication of metallic nanostructures[3–8] has led to a resurgence of interest in the linear and nonlinear optical properties of these field structures,[9–14] in their potential for applications in sensing,[7,15,16] and more generally in their application as elements of optical devices.[17–19] In standard introductions to surface plasmons, one envisions a semi-infinite metal bounded by an isotropic cladding [respectively, with relative dielectric constants ε_m (with negative real part) and ε_c (real and positive) at the frequency of interest] and looks for a solution of Maxwell's equations and the associated *saltus* (boundary) conditions where the fields are confined to the region near the interface.[20,21] As is well known, for *p*-polarized light a solution exists for fields characterized by a wave vector in the plane of the surface with magnitude κ, where

$$\kappa = \frac{\omega}{c}\sqrt{\frac{\varepsilon_c \varepsilon_m}{\varepsilon_c + \varepsilon_m}}. \tag{1}$$

If loss is neglected and ε_m taken to be real and negative, the resulting κ is real. That is, the field excitation could propagate forever along the surface; κ necessarily lies "outside the light line" of the cladding ($\kappa > \omega\sqrt{\varepsilon_c}/c$) so that the field is evanescent in the cladding and cannot be radiated away. In the presence of loss, always a feature in metal structures, ε_m acquires a positive imaginary part and so does κ, moving into the complex plane where its imaginary part describes the decrease in the surface plasmon field amplitude, due to absorption in the metal, as it propagates along the interface.

Such an idealized interface structure does not allow for the coupling of incident light into the surface plasmon. Traditional Otto and Kretschmann structures[22,23] are perhaps the simplest that make that possible. In the latter, a layer of metal with a thickness on the order of 50 nm, bounded above by a cladding, is placed above a substrate with a large refractive index. A field incident from the substrate with $\kappa > \omega\sqrt{\varepsilon_c}/c$ can, roughly speaking, tunnel through the metal and, near a particular angle of incidence, excite a surface plasmon at the metal/cladding interface. More formally, the surface plasmon nominally at the metal/cladding interface becomes leaky due to this tunneling with its κ acquiring an imaginary part even were loss absent. The excitation of the surface plasmon by incident radiation in the substrate leads to large fields near the metal/cladding interface, which in the presence of ubiquitous absorption in the metal leads to a dip in the reflectivity of the light incident from the substrate. This dip can be taken as an operational signature of the surface plasmon. Indeed, it is the presence of this dip and its sensitivity to adsorbates at the metal/cladding interface that is the basis of a major commercial application of surface plasmons in biosensing.[15]

The generalization of this scenario to metal spheres, nanowires, rods, and other shapes, and to a range of dielectric environments, is the focus of much of the recent work in plasmonics.[5,24,25] More recently, studies have also explored planar structure when the cladding is anisotropic (see Fig. 1).[26–30] Claddings with large birefringence are not unrealistic and could be constructed by using polymers or by exploiting form birefringence in nanostructured materials.[31] Elser and Podolskiy[30] have considered the case of a uniaxial cladding

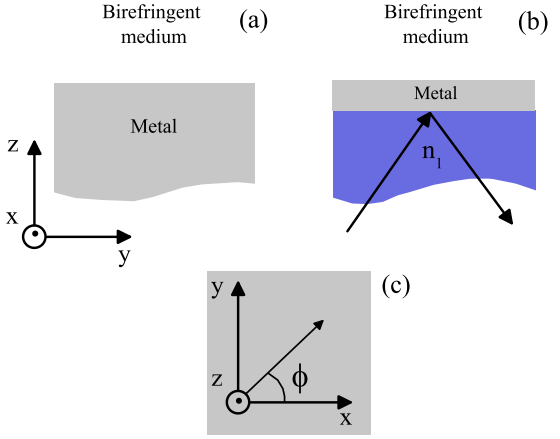

FIG. 1. (Color online) (a) Scheme of the metal/dielectric interface; (b) The Kretschmann configuration for surface plasmon detection; (c) top view of the interface. The angle between the in-plane wave vector and the $\hat{\mathbf{x}}$ axis is also shown.

where the optical axis is orthogonal to the metal/cladding interface. Here surface plasmon propagation is still isotropic in the plane, but ordinary and extraordinary indices can be used to tune the plasmon field profile and the propagation wave vector, almost independently.

For a biaxial cladding, or a uniaxial cladding where the optical axis lies in the plane of the interface, the situation is considerably more complicated. These scenarios are the focus of this study. Here the magnitude of the wave vectors that characterize surface plasmon propagation will depend on the direction of the wave vector in the plane of the interface; thus surface plasmon propagation becomes anisotropic in the plane of the interface, depending on the angle ϕ the wave vector forms with the x axis of the laboratory reference frame [see Fig. 1(c)].

Even for a uniaxial cladding we will see that the situation is qualitatively different depending on whether there is positive or negative birefringence ($n_e - n_o > 0$ or $n_e - n_o < 0$, respectively, where n_e and n_o are the extraordinary and ordinary refractive indices of the cladding). As well, the polarization (s or p) is no longer generally conserved upon reflection from the cladding at the metal/cladding interface; except at special ϕ, the waves that exist in the birefringent medium have components of both polarizations, and p-polarized field excitations in the metal can couple to both polarizations in the cladding. Finally, at any ϕ there are generally *two* light lines of the cladding, since the medium is birefringent.[32] An interesting question is whether or not some sort of surface plasmon excitation, only quasiguided, could lie outside one light line but inside the other.

In principle the identification of surface plasmon dispersion relations in these anisotropic systems could be undertaken in the same manner as in the traditional isotropic system. One would write down the Maxwell equations and the saltus conditions and look for solutions confined to the plane of the interface. However, the equation that results, which implicitly identifies the dispersion relation of any surface plasmon, is much more complicated. Li *et al.*[28] performed a study along these lines, but only considered excitations that might exist *outside both light lines*. In the lossless limit such excitations could propagate indefinitely. But it is not clear that in any real application these leakyless excitations would be more useful than excitations that might lie within one light line and be only quasiguided, for in any case both types of excitations would suffer significant loss due to absorption in the metal.

Ideally one might seek a more general set of relations $\kappa(\phi)$ (with κ necessarily complex) that identify solutions of Maxwell's equations that are confined largely to the interface, but perhaps leaking slightly into the cladding. This is much more complicated than the restricted problem considered by Li *et al.* Because of singularities at the light lines, it is not easy to find simple equations that are always valid, even for a uniaxial cladding; the biaxial case is almost algebraically prohibitive. And in case, the complicated equations that would result would not directly be of much use. Even in the simple isotropic case, where the surface plasmon dispersion relation in Eq. (1) can easily be written down, the interest in the field structure and its usefulness is due to the large fields that can actually be excited in structures such as that of Kretschmann, rather than in the surface plasmon behavior at the artificial, idealized interface between two semi-infinite media.

This suggests the strategy we adopt in this paper. As a general study of surface plasmons in the presence of anisotropic claddings, we calculate the dips in reflectivity that would be seen in an experiment using the structure of Kretschmann, where an anisotropic cladding is placed above a metal layer. These dips can be taken as operational signatures of the surface plasmons. More importantly, they indicate under what circumstances the field enhancement at the metal/cladding interface is large, indicating the situations in which surface plasmons play a major role in determining the optical properties of the structure and are therefore of primary physical interest. By this approach we can explore the whole of wave-vector space, inside and outside the light lines. For a uniaxial medium, we confirm the results of Li *et al.* outside both light lines, but identify hitherto unexplored field structures within the outer light line. These fields are quasiguide modes, and they result from the hybridization of an evanescent wave and a propagating wave in the birefringent. Even in the absence of losses they would be leaky due to radiation into the birefringent medium. For a biaxial medium we present what we believe is the first study, in either numerical or analytical form, of the excitation of a Kretschmann structure. For certain biaxial media we find that quasiguided modes propagating in almost all direction exist. As we explore the possible angles of excitation from the high-index substrate, we identify regions of parameter space where a field structure at the metal/cladding interface of one type changes its nature and almost blends into another; this kind of characterization would be difficult to achieve with a purely analytic set of solutions. Perhaps most significant is that these calculations, which provide a "bird's-eye" view of the excitation of the metal/cladding interface as the direction of incidence in the substrate is changed, identify the major physical features of that excitation over all parameter space, and point the way to topics that are worthy of further exploration.

In Sec. II we start by considering the case of a uniaxial medium. First we present equations for the light lines and describe analytically the surface plasmon properties along the propagation directions of maximum symmetry. Finally, we numerically study the surface plasmon properties along all the other directions. In Sec. III we generalize our results to the case of biaxial media, and in Sec. IV we present our conclusions. Throughout the paper we assume that the birefringent dielectrics we consider are lossless.

II. UNIAXIAL MEDIA

We first consider a uniaxial dielectric medium with its optical axis laying along the $\hat{\mathbf{x}}$ direction. The relative dielectric tensor then takes the form

$$\varepsilon = \begin{pmatrix} \varepsilon_e & 0 & 0 \\ 0 & \varepsilon_o & 0 \\ 0 & 0 & \varepsilon_o \end{pmatrix}, \tag{2}$$

where ε_o and ε_e are the relative ordinary and extraordinary dielectric constants, respectively.

Since the medium is birefringent, for a given frequency ω and a real wave-vector component κ in the xy plane there exist two possible waves, characterized by two different possible z components w_i of the wave vector; each of these w_i satisfies the equation[32]

$$[\varepsilon_o(\kappa_y^2 + w^2) + \varepsilon_e(\kappa_x^2 + \varepsilon_o k_0^2)](\kappa_x^2 + \kappa_y^2 + w^2 - \varepsilon_o k_0^2) = 0, \tag{3}$$

where κ_x and κ_y are the indicated wave-vector components in the (xy) plane. From Eq. (3) we get

$$w_1^2 = \varepsilon_o k_0^2 - \kappa_x^2 - \kappa_y^2, \tag{4}$$

$$w_2^2 = \varepsilon_e k_0^2 - \frac{\varepsilon_e}{\varepsilon_o}\kappa_x^2 - \kappa_y^2, \tag{5}$$

where $k_0 = \omega/c$.

We can find the values of $\kappa = (\kappa_x, \kappa_y)$ at which the w_i vanish. These points are solutions of

$$\frac{\kappa_x^2}{\varepsilon_o k_0^2} + \frac{\kappa_y^2}{\varepsilon_o k_0^2} = 1, \tag{6}$$

$$\frac{\kappa_x^2}{\varepsilon_o k_0^2} + \frac{\kappa_y^2}{\varepsilon_e k_0^2} = 1 \tag{7}$$

which describe, respectively, a circle and an ellipse in the (κ_x, κ_y) plane. They define the so-called "light lines," identifying the electromagnetic excitations in an infinite medium with the fields that are independent of z. In the case of a uniaxial material, for which $\varepsilon_o \neq \varepsilon_e$, there are two qualitatively different situations, shown in Figs. 2(a) and 2(b), corresponding to negative and positive birefringence, respectively. Recall that the birefringence sign is characterized by the difference $\delta_e = \varepsilon_e - \varepsilon_o$. In other words, we talk about positive (negative) birefringence when the extraordinary refractive index is larger (smaller) than the ordinary one.

With our assumption of a lossless birefringent medium, the w_i that result from Eqs. (4) and (5) more generally are either purely real or purely imaginary. The circle and the ellipse in Figs. 2(a) and 2(b) divide the (κ_x, κ_y) plane into three regions. (i) The internal one, where $\mathrm{Re}(w_i) \neq 0$ for both w_i, and thus a field with a wave-vector component κ in the (xy) plane can propagate in the dielectric medium with one of two possible real wave-vector components along z. (ii) An intermediate region, for which one of the two waves is evanescent. (iii) The external zone, where both w_1 and w_2 are purely imaginary, and thus all fields must be evanescent in the cladding.

We now consider this lossless birefringent medium above a metal (see Fig. 1). It has been shown that hybridized surface plasmons can exist in the region outside both light lines [i.e., in region (iii)],[28] but to date the question of whether or not waves that are evanescent and propagating in the z direction can coexist in region (ii) has not been considered.

First we consider possible surface excitations with wave vectors κ in the plane directed along $\pm\hat{\mathbf{x}}$ and $\pm\hat{\mathbf{y}}$, the directions associated with the principal axes of the dielectric tensor. Here the solutions of Maxwell's equations are odd or even under reflection with respect to the plane $xz(yz)$ for κ in the $\pm\hat{\mathbf{x}}(\pm\hat{\mathbf{y}})$ direction. This allow us to classify any mode as either transverse electric (TE) or magnetic (TM) with respect to the plane defined by the propagation direction and $\hat{\mathbf{z}}$. For these special directions the surface plasmon is TM polarized and its dispersion relation can be calculated analytically.[30]

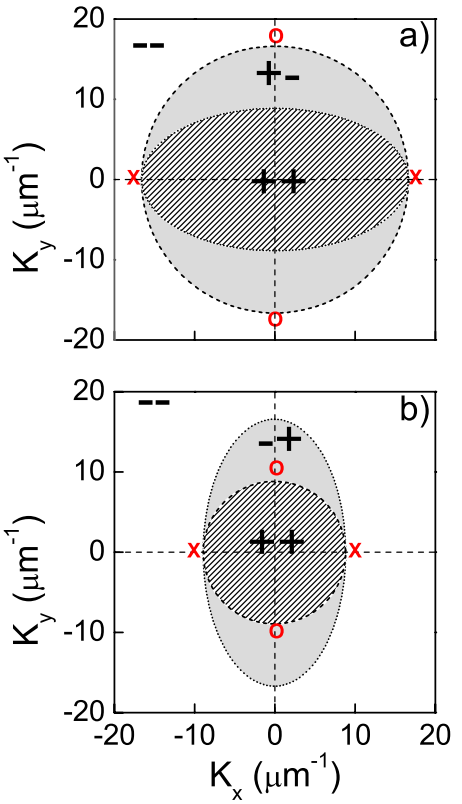

FIG. 2. (Color online) The behavior of w_i^2 for uniaxial media. The (κ_x, κ_y) plane is divided in three regions on the basis of the sign of w_i^2: both positive (patterned), both negative (white), and one positive and one negative (gray). Plots are made for $\lambda = 2\pi/k_0 = 1$ μm. Two cases are considered: (a) negative birefringence ($\varepsilon_e = 2$ and $\varepsilon_o = 7$); (b) positive birefringence ($\varepsilon_e = 7$ and $\varepsilon_o = 2$). The circle (dashed) and the ellipse (dotted) represent the two light lines described by Eqs. (6) and (7), respectively. We show the position of the ordinary (O) and the extraordinary (X) surface plasmons along the symmetry directions, when the dielectric is used as a cladding above a lossless metal.

In particular, when the surface plasmon propagates along $\pm\hat{\mathbf{y}}$, we have

$$\kappa_{ORD} = k_0 \sqrt{\frac{\varepsilon_o \varepsilon_m}{\varepsilon_o + \varepsilon_m}}, \tag{8}$$

where ε_m is the metal dielectric function. We call this the *ordinary surface plasmon*, as its dispersion relation is that one would have by considering an interface between a metal and an isotropic medium of dielectric function ε_o. Indeed, the properties of the surface plasmon are uniquely determined by the ordinary wave with wave-vector components satisfying $w_1^2 = \varepsilon_o k_0^2 - \kappa_y^2$ [cf. Eq. (4)].

If instead we consider a solution with κ in the $\pm\hat{\mathbf{x}}$ direction, the surface plasmon dispersion relation is slightly more complicated

$$\kappa_{EXT} = k_0 \sqrt{\frac{\varepsilon_o \varepsilon_m (\varepsilon_e - \varepsilon_m)}{\varepsilon_o \varepsilon_e - \varepsilon_m^2}}. \tag{9}$$

We call this the *extraordinary surface plasmon*, since this dispersion relation reflects the material anisotropy and, in particular, it involves the "extraordinary" wave, with wavevector components satisfying $w_2^2 = \varepsilon_e k_0^2 - \varepsilon_e \kappa_x^2 / \varepsilon_o$ [cf. Eq. (5)].

It follows immediately that, if $\varepsilon_o = \varepsilon_e$, Eqs. (8) and (9) coincide. It is worth noting that κ_{ORD} and κ_{EXT} diverge at the frequencies satisfying $\varepsilon_o + \varepsilon_m = 0$ and $\varepsilon_o \varepsilon_e - \varepsilon_m^2 = 0$, respectively. As the frequency is varied and these conditions are approached, the simultaneous existence of ordinary and extraordinary plasmons in their respective directions is not guaranteed.[28] Although this is an interesting situation, in the following we always consider frequencies at which both ordinary and extraordinary plasmons exist. That is, we assume we are at frequencies far from the metal plasma frequency, and so

$$|\varepsilon_m| \gg \varepsilon_o \quad \text{and} \quad |\varepsilon_m| \gg \sqrt{\varepsilon_o \varepsilon_e}, \tag{10}$$

as usually holds for typical metals and dielectrics at frequencies in the visible and infrared.

Let us identify the position of the ordinary and the extraordinary surface plasmons in the (κ_x, κ_y) plane, with respect to the light lines shown in Fig. 2. We can strictly do this only where ε_m is assumed to be real, so that the resulting κ_{ORD} and κ_{EXT} are real; for the moment we make this assumption. Then the ordinary plasmons lie on the axis defined by $\kappa_x = 0$ at the positions $\kappa_y = \pm \kappa_{ORD}$, while the extraordinary has $\kappa_y = 0$ and $\kappa_x = \pm \kappa_{EXT}$. When Eq. (10) is satisfied we can show that the effective dielectric function of the ordinary and extraordinary plasmons are larger than ε_o. That is,

$$\frac{\varepsilon_o \varepsilon_m}{\varepsilon_o + \varepsilon_m} > \varepsilon_o, \quad \frac{\varepsilon_o \varepsilon_m (\varepsilon_e - \varepsilon_m)}{\varepsilon_o \varepsilon_e - \varepsilon_m^2} > \varepsilon_o. \tag{11}$$

In other words, the ordinary and the extraordinary plasmons are always beyond the ordinary light line [i.e., the circle of radius $k_0 \sqrt{\varepsilon_o}$ described by the Eq. (6)], independently of the birefringence value.

In contrast, the surface plasmon position with respect to the extraordinary light line [that is, the ellipse of Eq. (7)] depends strongly on the value of the birefringence δ_ε. In particular, an interesting question is whether or not there are birefringence values such that

$$\frac{\varepsilon_o \varepsilon_m}{\varepsilon_o + \varepsilon_m} < \varepsilon_e. \tag{12}$$

This is the condition for the ordinary surface plasmon to lie *within* the extraordinary light line. Since the birefringence $\delta_\varepsilon = \varepsilon_e - \varepsilon_o$, this condition holds whenever $\delta_\varepsilon > \delta_0$, where the critical birefringence δ_0 is given by

$$\delta_0 \equiv \frac{-\varepsilon_o^2}{\varepsilon_o + \varepsilon_m}. \tag{13}$$

Hence for a large enough positive birefringence the ordinary surface plasmon lies in the region between the ordinary and the extraordinary light lines (i.e., those identified by the circle and the ellipse). For these values of κ the extraordinary wave in the birefringent medium can propagate in the z direction [see Fig. 2(b)] and is TE polarized. That is, the ordinary surface plasmon can exist at a particular $\kappa = |\boldsymbol{\kappa}|$ while, in other directions but a the same $\kappa = |\boldsymbol{\kappa}|$, there exist waves that propagate in the birefringent medium.

If an imaginary part of ε_m is restored, then κ_{ORD} and κ_{EXT} acquire imaginary components, and the best we can do to indicate the presence of the surface excitations in the κ plane is to plot their real parts in diagrams such as Fig. 2. Nonetheless, the qualitative behavior of the positions of the surface plasmons in the κ plane that we found above still holds.

Let us now consider all the other propagation directions for which we do not have a simple analytic theory. In order to investigate the existence and the properties of surface plasmons we use an exact coupled wave analysis that is able to deal with the dielectric medium anisotropy, and where the metal absorption is taken into account by considering its complex dielectric function.[33–35] We study the surface plasmons by calculating the attenuated total reflectance (ATR) spectrum with light incident from an isotropic substrate with a high index n_1 in the Kretschmann configuration [see Fig. 1(b)]. When the in-plane momentum $\kappa = (\kappa_x, \kappa_y)$ of the incident beam is close to the real component of the surface plasmon wave vector, an attenuation of the reflectance is expected due to the absorption enhancement associated with the surface plasmon excitation. In an actual experiment, κ could be varied while holding the incident wavelength fixed, simply by changing the direction of the incident beam in the substrate, varying both its angle of incidence and its direction projected onto the (xy) plane.[23]

Although the qualitative nature of our results is rather general, we present calculations only for particular sets of parameters. We always consider a 50-nm-thick gold layer [$\varepsilon = -42.081 + 2.9i$ at a vacuum wavelength of $\lambda = 1$ μm (Ref. 35)] and a high-index substrate having a real dielectric constant $\varepsilon_1 = n_1^2 = 12$. We do not choose any particular material for the birefringent medium, but the values of 7 and 2 that we adopt for the dielectric constants are realistic and can be obtained either by using strained polymers or by exploiting form birefringence in nanostructured materials.[31,36–38]

The calculated unpolarized ATR spectra for a TM-polarized incident field[39] is shown in Fig. 3 for an isotropic cladding, and in Figs. 4(a) and 4(b) for a negative birefringent medium and a positive birefringent medium, respectively. For a given propagation direction, defined by $\phi = \text{atan}(\kappa_x / \kappa_y)$, the dip in the reflectance spectrum as κ is varied is associated with absorption enhancement due to surface plasmon excitation. For an isotropic cladding (see Fig. 3), the reflectance minimum describes a circle whose radius is essentially the real part of ordinary plasmon propagation wave vector; the reflectance spectrum is independent of ϕ. In contrast with this is Fig. 4(a). In the presence of negative

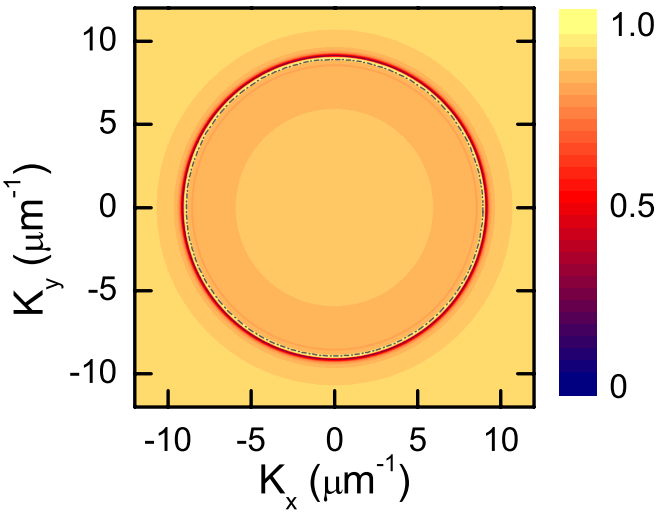

FIG. 3. (Color online) Total reflectance in the Kretschmann configuration as a function of κ_x and κ_y in the case of an isotropic cladding with $\varepsilon_e=\varepsilon_o=2$. We consider TM-polarized incident light at wavelength $\lambda=1$ μm, and $\varepsilon_m=\varepsilon_{gold}\simeq-42.081+2.9i$ (Ref. 35). The dash-dotted line indicates the cladding light line ($w_1^2=w_2^2=0$).

birefringence, we observe a reflectance dip described by a curve that is slightly squeezed in along $\kappa_y=0$, where the dip corresponds to the extraordinary surface plasmon resonance. Along all other propagation directions, the surface plasmon is *polarization hybridized* and is characterized by four evanescent waves (two in the metal and two in the birefringent medium) having the same in-plane component but different polarizations and exponentially decays from the interface as shown in Li *et al.*[28]

We now consider a cladding with positive birefringence [Fig. 4(b)], where the ATR spectrum is qualitatively different. If we look at the zoom shown in Fig. 5, the most interesting result is the presence of a narrow reflectance dip in the region between the ordinary and the extraordinary light lines. As we have seen earlier, in this region only one of the two waves in the birefringent medium is evanescent and confined to the interface; the other has a real wave-vector component in the z direction. Therefore, the surface plasmon here is the result of the hybridization of evanescent and propagating waves. This means that it is not a truly guided mode but rather a mode *leaking* into the birefringent cladding (except in the $\pm\hat{\mathbf{y}}$ direction along which the surface plasmon is not hybridized).

The situation can be understood better by looking at the field distributions along z resulting from TM-polarized excitation from the high-index dielectric at the angle corresponding the minimum of the reflectance, which we take to identify surface plasmon resonance. In Fig. 6 we plot such profiles for different in-plane propagation directions, indicated in Fig. 5 and defined by the azimuthal angle ϕ. In Fig. 6(a) we show the squared norm of the (total) complex amplitude of field distribution resulting from excitation at $\phi=0°$, where we can excite the extraordinary surface plasmon. As it is expected, the curve is exponentially decreasing in both metallic and dielectric media. If we move to $\phi=30°$, the situation is different. Although the absolute maximum of the

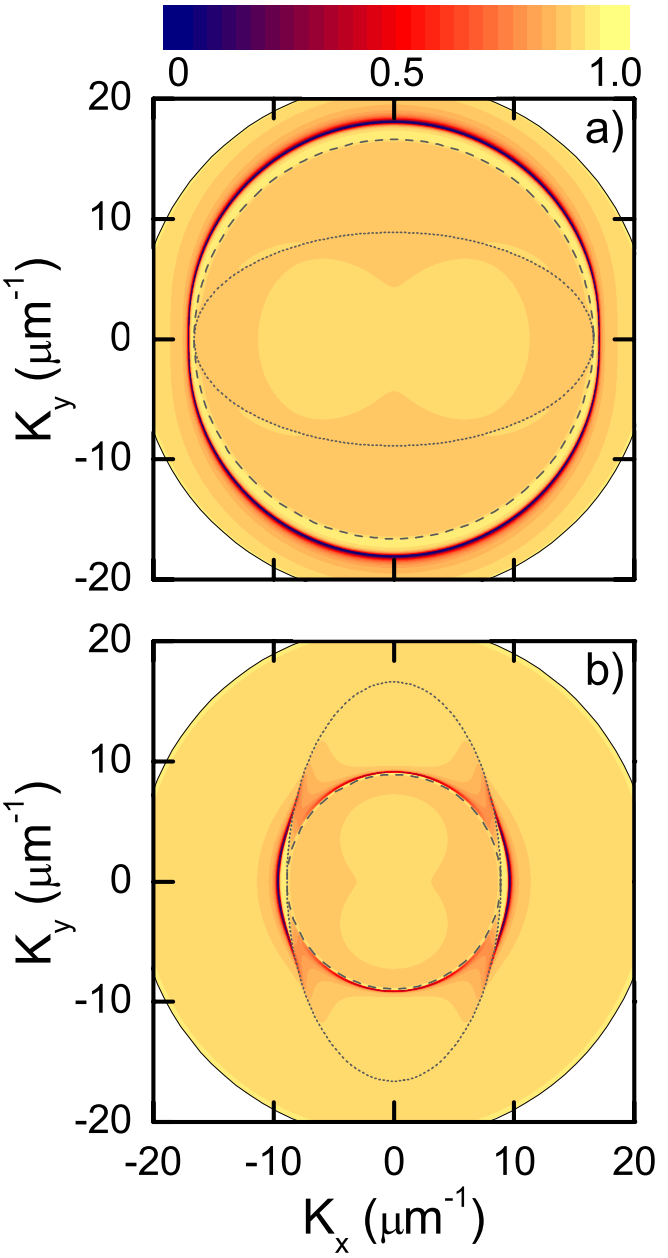

FIG. 4. (Color online) Total reflectance in the Kretschmann configuration as a function of κ_x and κ_y for (a) negative birefringence ($\varepsilon_e=2$ and $\varepsilon_o=7$) and (b) positive birefringence ($\varepsilon_e=7$ and $\varepsilon_o=2$). We consider TM-polarized incident light at wavelength $\lambda=1$ μm, and $\varepsilon_m=\varepsilon_{gold}\simeq-42.081+2.9i$ (Ref. 35). The circle (dashed) and the ellipse (dotted) are the two cladding light lines described by Eqs. (6) and (7), respectively. The solid line corresponds to the maximum in-plane momentum that can be accessed by excitation from a high-index substrate with $\varepsilon_1=12$.

field is still at the metal/dielectric interface, the curve is not purely exponentially decaying, but there is a relative maximum inside the birefringent material. Note that the surface plasmon resonance is beyond the two light lines, so except for leakage through the interface of the metal and the high-index substrate the surface plasmon is a truly guided mode, but it is the result of the hybridization of the ordinary and the extraordinary waves. This means that the field in the metal

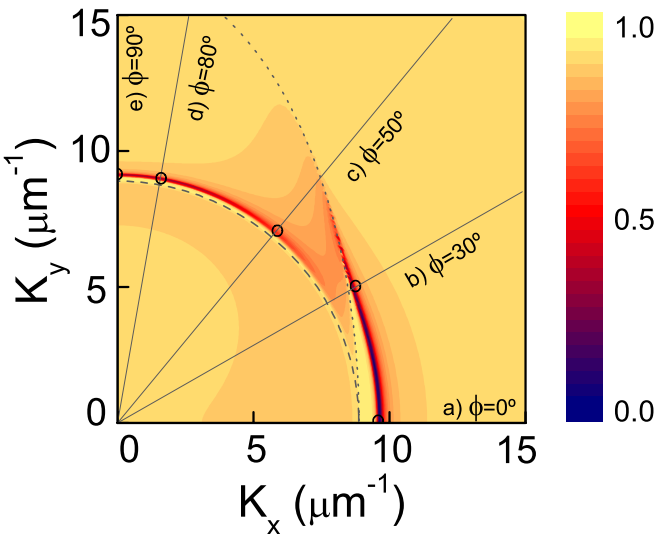

FIG. 5. (Color online) Detail of the total reflectance reported in Fig. 4(b), calculated in the Kretschmann configuration as a function of κ_x and κ_y for positive birefringence ($\varepsilon_e=7$ and $\varepsilon_o=2$). We consider TM-polarized incident light at wavelength $\lambda=1$ μm, and $\varepsilon_m=\varepsilon_{gold}\simeq-42.081+2.9i$ (Ref. 35). The dashed and the dotted curves are the two cladding light lines described by Eqs. (6) and (7), respectively. The small circles indicate the points at which we perform the calculation of the field distributions shown in Fig. 6.

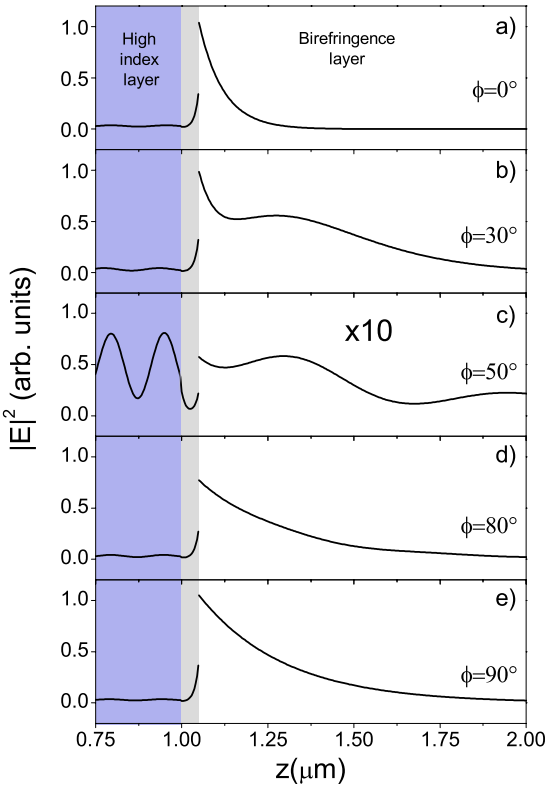

FIG. 6. (Color online) Squared modulus of the complex electromagnetic field amplitude for a TM-polarized incident beam resonantly coupled to the surface plasmon in the Kretschmann configuration for the propagation angles (a) $\phi=0°$, (b) $\phi=30°$, (c) $\phi=50°$, (d) $\phi=80°$, and (e) $\phi=90°$. We consider TM-polarized incident light at wavelength $\lambda=1$ μm, $\epsilon_1=12$, $\varepsilon_m=\varepsilon_{gold}\simeq-42.081+2.9i$ (Ref. 35), $\varepsilon_e=7$ and $\varepsilon_o=2$.

and dielectric medium is a superposition *two* different evanescent waves.[28,29] The profile is reminiscent of a D'yakonov wave, which can propagate at the interface between two dielectric media if one of them is birefringent.[40] Although D'yakonov waves are usually studied in the absence of absorption, unlike in our system where absorption in the metal is present, the origin of such a maximum is identical, and it is associated with the hybridized nature of the two modes. We consider now $\phi=50°$ (see Fig. 5), where the surface plasmon excitation is inside one of the two light lines. Here the situation is qualitatively different. The squared modulus of the complex-field amplitude [see Fig. 6(c)], while characterized by an exponentially decaying envelope function, is oscillating. As for the excitation at $\phi=30°$ there is a hybridization between two distinct waves allowed in the birefringent medium, but here one is evanescent and one is propagating. The quasiguided nature of the propagating mode is manifest in the oscillations in the birefringent cladding. As we move to $\phi=80°$, the oscillation of the field amplitude in the birefringent medium is suppressed and the field is almost exponentially decaying. This indicates that the ordinary wave becomes dominant in the hybridization as we approach the symmetry direction $\hat{\mathbf{y}}$, although the reflectance dip is still inside one of the light lines. Finally, at $\phi=90°$, we recover the typical profile of the ordinary surface plasmon excitation.

III. BIAXIAL MEDIA

In this section we generalize the results presented above to the more complicated configuration where the cladding is a biaxial medium, with a dielectric tensor of the form

$$\varepsilon=\begin{pmatrix}\varepsilon_x & 0 & 0\\ 0 & \varepsilon_y & 0\\ 0 & 0 & \varepsilon_z\end{pmatrix}, \tag{14}$$

in the laboratory reference frame, where we take $\varepsilon_x\neq\varepsilon_y\neq\varepsilon_z$ to avoid the limits of isotropic and uniaxial materials that have just been investigated. As in the previous section, we start our discussion by studying the properties of the light lines of the birefringent medium. For a given propagation direction in the xy plane, there are again two waves in the dielectric material. The expression for the wave vector z-components w_1 and w_2 are, in general, more complicated than those of Eqs. (4) and (5); they have been presented by Abdulhalim.[41] Yet, the equations for the light lines, which are determined by the condition that at least one of the w_i vanishes, can be easily found[32]

$$\frac{\kappa_x^2}{\varepsilon_z k_0^2}+\frac{\kappa_y^2}{\varepsilon_z k_0^2}=1, \tag{15}$$

$$\frac{\kappa_x^2}{\varepsilon_y k_0^2}+\frac{\kappa_y^2}{\varepsilon_x k_0^2}=1. \tag{16}$$

These equations describe a circle and an ellipse in the (κ_x,κ_y) plane, respectively. As for a uniaxial cladding, the

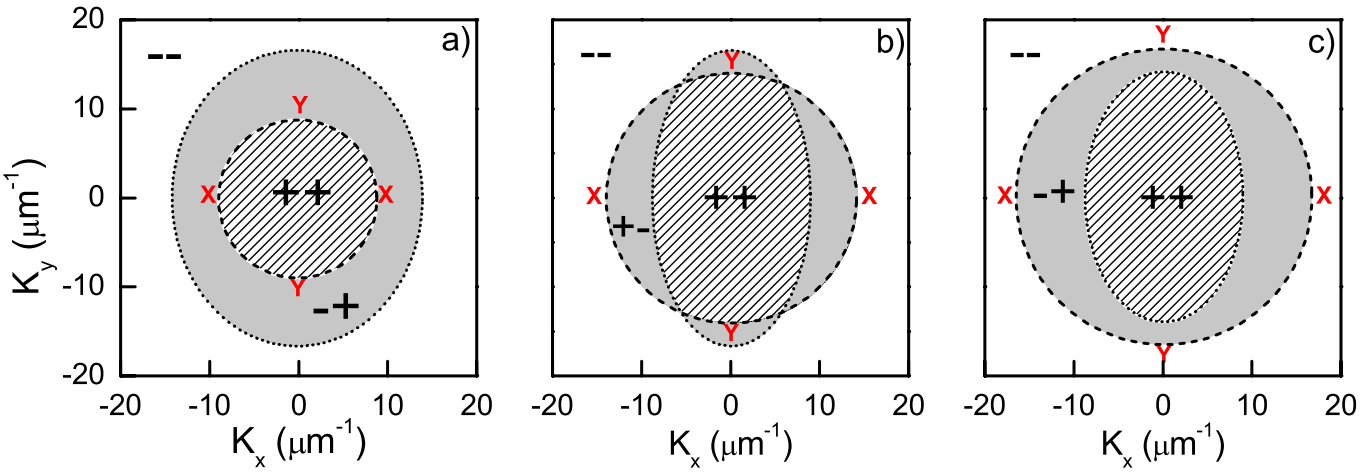

FIG. 7. (Color online) The behavior of w_i^2 for biaxial media. The (κ_x, κ_y) plane is divided in three regions on the basis of the sign of w_i^2: both positive (patterned), both negative (white), and one positive and one negative (gray). Plots are made for $\lambda = 2\pi/k_0 = 1$ μm. Three qualitatively different situations are studied: (a) $(\varepsilon_x, \varepsilon_y > \varepsilon_z)$ with $\varepsilon_x = 7$, $\varepsilon_y = 5$, and $\varepsilon_z = 2$; (b) $(\varepsilon_x, \varepsilon_z > \varepsilon_y)$ with $\varepsilon_x = 7$, $\varepsilon_y = 2$, and $\varepsilon_z = 5$; and (c) $(\varepsilon_z > \varepsilon_x, \varepsilon_y)$ with $\varepsilon_x = 5$, $\varepsilon_y = 2$, and $\varepsilon_z = 7$. The circle (dashed) and the ellipse (dotted) are the two light lines described by Eqs. (15) and (16), respectively. We show the positions of the surface plasmon resonances along the direction of high-symmetry $\hat{\mathbf{x}}$ and $\hat{\mathbf{y}}$, when the dielectric is used as a cladding above a lossless metal.

two curves divide the (κ_x, κ_y) plane into regions that satisfy one of three conditions: two, one, or no waves with real z components exist. Since a real (imaginary) w_i is associated with propagation (evanescence) in the z direction, we refer to the condition that there is only one real z component (and hence one imaginary) as the "coexistence condition," indicating the coexistence of propagating and evanescent waves. We refer to a region in the (κ_x, κ_y) plane where the coexistence condition is satisfied as a "coexistence region."

Depending on the choice of ε_x, ε_y, and ε_z, there are only three qualitatively different scenarios: (a) $\varepsilon_x, \varepsilon_y > \varepsilon_z$, (b) $\varepsilon_x, \varepsilon_z > \varepsilon_y$, and (c) $\varepsilon_z > \varepsilon_x, \varepsilon_y$. These three situations are shown in Fig. 7, where we take $\varepsilon_x, \varepsilon_y, \varepsilon_z \in \{2, 5, 7\}$. Since we consider $\varepsilon_x \neq \varepsilon_y \neq \varepsilon_z$, the circle and the ellipse are not tangent, as they were for a uniaxial cladding where we took $\varepsilon_y = \varepsilon_z$. The situations (a), (b), and (c) identified above are characterized by subdivisions of the (κ_x, κ_y) plane that are, in general, different than those shown in Fig. 2. In particular, in Figs. 7(a) and 7(c) [situations (a) and (c)], there is a single coexistence region in the plane, while in case (b) there are four distinct coexistence regions. Thus situation (b) is similar but more complicated than that for a uniaxial crystal with positive birefringence [Fig. 2(b)], where there are two distinct coexistence regions. The shape and number of coexistence regions affect the propagation properties of the surface plasmons, as we see below.

Turning now to the structure shown in Fig. 1(a), but for a biaxial cladding, we determine the positions of the surface plasmon resonances along the directions of maximum symmetry $\pm\hat{\mathbf{x}}$ and $\pm\hat{\mathbf{y}}$. As in our discussion of a uniaxial cladding, we begin by assuming the dielectric constant of the metal is real. Then in the maximum-symmetry directions it is easy to identify analytic expressions for the surface plasmon dispersion relations. We indicate these solutions by *SPX* and *SPY*, where *X* and *Y* identify the surface plasmon propagation direction. The dispersion relations are those of two extraordinary surface plasmons [see Eq. (9)], where

$$\kappa_{SPX} = k_0 \sqrt{\frac{\varepsilon_z \varepsilon_m (\varepsilon_x - \varepsilon_m)}{\varepsilon_z \varepsilon_x - \varepsilon_m^2}}, \tag{17}$$

$$\kappa_{SPY} = k_0 \sqrt{\frac{\varepsilon_z \varepsilon_m (\varepsilon_y - \varepsilon_m)}{\varepsilon_z \varepsilon_y - \varepsilon_m^2}}. \tag{18}$$

As in our study of a uniaxial cladding we assume we are at a frequency well below the plasma frequency, and so

$$|\varepsilon_m| \gg \sqrt{\varepsilon_i \varepsilon_k} \quad \text{with} \quad i, j, k = x, y, z. \tag{19}$$

In this approximation

$$\kappa_{SPi} = k_0 \sqrt{\frac{\varepsilon_z \varepsilon_m (\varepsilon_i - \varepsilon_m)}{\varepsilon_z \varepsilon_i - \varepsilon_m^2}} \sim k_0 \sqrt{\varepsilon_z}, \tag{20}$$

and the positions of the resonances are indicated by X and Y in Figs. 7(a)–7(c). These are very close to the light line defined by $\kappa_x^2 + \kappa_y^2 = \omega^2 \varepsilon_z / c^2$. In particular, in Fig. 7(a) the surface plasmon resonances in all high-symmetry directions are in the coexistence region; in Fig. 7(b) only two are in the coexistence regions; and in Fig. 7(c) none are.

The analysis of surface plasmons in the other propagation directions is done, following our treatment of a uniaxial cladding in the preceding section, by means of a coupled wave analysis. Again we assume the Kretschmann configuration shown in Fig. 1(b), with a 50-nm-thick gold layer with $\varepsilon_m = -42.081 + 2.9i$ (Ref. 35) and a high-index substrate with a real dielectric constant $\varepsilon_1 = n_1^2 = 12$. The ATR spectra for the three cases described in Fig. 7 are shown in Fig. 8, where we can see that along other propagation directions the surface

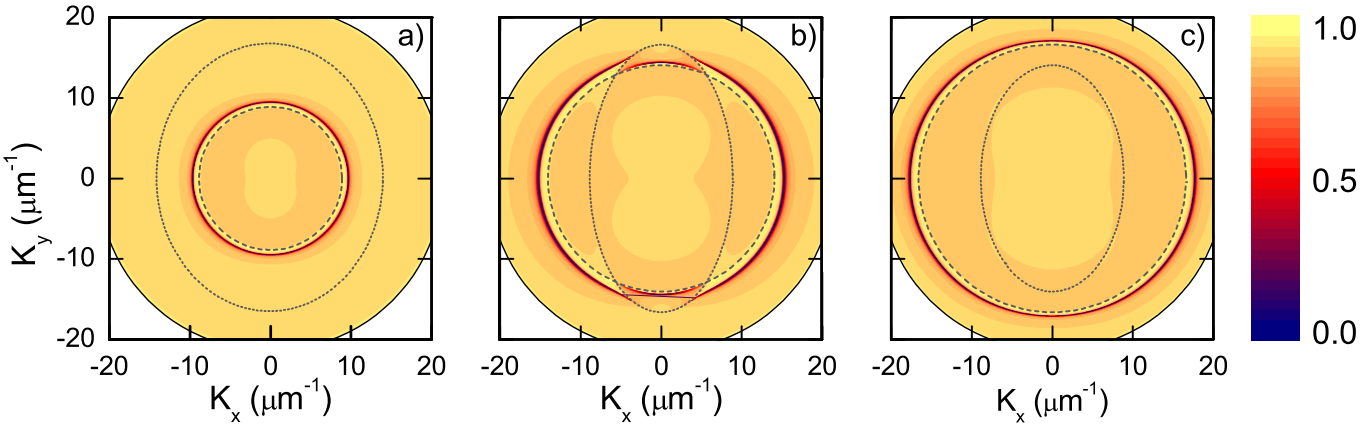

FIG. 8. (Color online) Total reflectance in the Kretschmann configuration as a function of κ_x and κ_y for (a) $(\varepsilon_x, \varepsilon_y > \varepsilon_z)$ with $\varepsilon_x=7$, $\varepsilon_y=5$, and $\varepsilon_z=2$; (b) $(\varepsilon_x, \varepsilon_z > \varepsilon_y)$ with $\varepsilon_x=7$, $\varepsilon_y=2$, and $\varepsilon_z=5$; and (c) $(\varepsilon_z > \varepsilon_x, \varepsilon_y)$ with $\varepsilon_x=5$, $\varepsilon_y=2$, and $\varepsilon_z=7$. We consider TM-polarized incident light at wavelength $\lambda=1$ μm, and $\varepsilon_m=\varepsilon_{gold}\simeq -42.081+2.9i$ (Ref. 35). The circle (dashed) and the ellipse (dotted) are the two cladding light lines described by Eqs. (15) and (16), respectively. The solid line corresponds to the maximum in-plane momentum that can be accessed by excitation from a high-index substrate with $\varepsilon_1=12$.

plasmon resonances are also close to the light line defined by Eq. (15).

As we found for a uniaxial cladding, the behavior of the surface plasmon resonances with a biaxial cladding are constrained by the position of the surface plasmon resonances along the high-symmetry directions $\pm\hat{\mathbf{x}}$ and $\pm\hat{\mathbf{y}}$. In particular, when *SPX* and *SPY* are both in a coexistence region [Fig. 8(a)] or in a region where both waves are evanescent in the z direction [Fig. 8(c)], the reflectance dip describes a single slightly elliptical curve. In contrast, if the *SPY* lies in a coexistence region but *SPX* does not [Fig. 8(b)], the curve associated with the dip corresponding to surface plasmon excitation has an interruption whenever it crosses the elliptical light line. Many of the features of the reflectance spectra of Fig. 8 are similar to those discussed in the previous section and can be understood by generalizing the concept of surface plasmon hybridization.

Nevertheless, the result shown in Fig. 8(a) is peculiar to a biaxial medium, as it is related to the fact that both *SPX* and *SPY* are in the sole coexistence region. The surface plasmon resonance dip is located entirely within this coexistence region, exists for all directions of propagation and is far from the ellipse describing the second light line. This structure is interesting since, excluding κ lying in the $\pm\hat{\mathbf{x}}$ and $\pm\hat{\mathbf{y}}$, the surface plasmon is leaky into the cladding in all directions, the result of the hybridization between evanescent and propagating waves. From the ATR spectrum alone, it is not possible to appreciate the amount of light lost because of metal absorption, and the amount lost because of transmission through the metal by the surface plasmon excitation. So we look at the corresponding transmittance spectrum, shown in Fig. 9. A transmittance close to the 30% is observed for almost all propagation directions in the (κ_x, κ_y) plane. Only around $\pm\hat{\mathbf{x}}$ and $\pm\hat{\mathbf{y}}$ are the low reflectances seen in the ATR calculation essentially entirely due to the absorption, as there is no hybridization between evanescent and propagating waves for $\kappa_x=0$ and $\kappa_y=0$.

IV. CONCLUSIONS

This study confirms the richness of physics at the interface of a metal and a birefringent dielectric cladding. Probably the most interesting result for a uniaxial cladding is the presence of a quasiguided surface plasmon excitation that can arise for positive birefringence, and which results from the hybridization of evanescent and propagating waves. For a biaxial cladding, if the principal dielectric constants associated with directions in the plane are greater than that associated with the direction normal to the interface, a quasiguided surface plasmon exists in all directions except those of high symmetry.

The coupled wave analysis presented here corresponds directly to what a standard ATR experiment would reveal and gives the opportunity to directly study the properties of the surface plasmon excitation by means of the calculation of reflectance spectra in a configuration that can be experimentally achieved and also to evaluate the field distributions associated with the surface plasmon excitation.

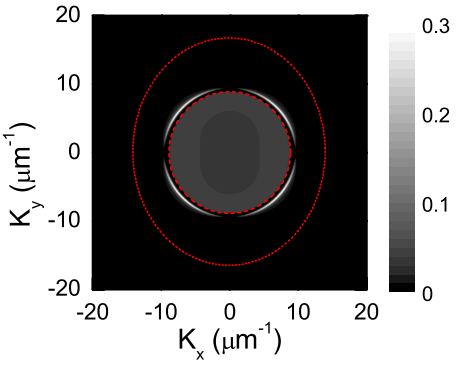

FIG. 9. (Color online) Total transmittance in the Kretschmann configuration as a function of κ_x and κ_y for $\varepsilon_x=7$, $\varepsilon_y=5$, and $\varepsilon_z=2$; We consider TM-polarized incident light at wavelength $\lambda=1$ μm, and $\varepsilon_m=\varepsilon_{gold}\simeq -42.081+2.9i$ (Ref. 35). The circle (red dashed) and the ellipse (red dotted) are the two cladding light lines described by Eqs. (15) and (16), respectively.

ACKNOWLEDGMENTS

We are grateful to M. Galli, D. Bajoni, and M. Patrini for useful discussions. Financial support from CNISM through the INNESCO initiative and from the Ontario Center of Excellence is acknowledged.

[1] R. A. Ferrell, Phys. Rev. **111**, 1214 (1958).
[2] R. E. Wilems and R. H. Ritchie, Phys. Rev. Lett. **19**, 1325 (1967).
[3] W. L. Barnes, A. Dereux, and T. W. Ebbesen, Nature (London) **424**, 824 (2003).
[4] P. Berini, G. Mattiussi, N. Lahoud, and R. Charbonneau, Appl. Phys. Lett. **90**, 061108 (2007).
[5] S. Lal, S. Link, and N. J. Halas, Nat. Photonics **1**, 641 (2007).
[6] I. De Leon and P. Berini, Phys. Rev. B **78**, 161401(R) (2008).
[7] F. De Angelis, M. Patrini, G. Das, I. Maksymov, M. Galli, L. Businaro, L. C. Andreani, and E. Di Fabrizio, Nano Lett. **8**, 2321 (2008).
[8] H. Raether, *Surface Plasmons* (Springer, New York, 1988).
[9] J. E. Sipe, Surf. Sci. **105**, 489 (1981).
[10] J. E. Sipe, V. C. Y. So, M. Fukui, and G. I. Stegeman, Phys. Rev. B **21**, 4389 (1980).
[11] J. Elliott, I. I. Smolyaninov, N. I. Zheludev, and A. V. Zayats, Phys. Rev. B **70**, 233403 (2004).
[12] M. I. Stockman, Phys. Rev. Lett. **93**, 137404 (2004).
[13] K. Li, X. Li, M. I. Stockman, and D. J. Bergman, Phys. Rev. B **71**, 115409 (2005).
[14] H. Mertens and A. Polman, Appl. Phys. Lett. **89**, 211107 (2006).
[15] J. Homola, Anal. Bioanal. Chem. **377**, 528 (2003).
[16] P. N. Prasad, *Introduction to Biophotonics* (Wiley, New York, 2003).
[17] J. A. Dionne, L. A. Sweatlock, H. A. Atwater, and A. Polman, Phys. Rev. B **73**, 035407 (2006).
[18] A. Polman, Science **322**, 868 (2008).
[19] S. Jetté-Charbonneau and P. Berini, Appl. Phys. Lett. **91**, 181114 (2007).
[20] W. L. Barnes, J. Opt. A, Pure Appl. Opt. **8**, S87 (2006).
[21] S. Maier, *Plasmonics: Fundamentals and Applications* (Springer, New York, 2007).
[22] A. Otto, Z. Phys. A: Hadrons Nucl. **216**, 398 (1968).
[23] E. Kretschmann, Z. Phys. A: Hadrons Nucl. **241**, 313 (1971).
[24] C. L. Nehl, N. K. Grady, G. P. Goodrich, F. Tam, N. J. Halas, and J. H. Hafner, Nano Lett. **4**, 2355 (2004).
[25] H. Wang, D. Brandl, F. Le, P. Nordlander, and N. J. Halas, Nano Lett. **6**, 827 (2006).
[26] I. Avrutsky, J. Opt. Soc. Am. A **20**, 548 (2003).
[27] A. A. Krokhin, A. Neogi, and D. McNeil, Phys. Rev. B **75**, 235420 (2007).
[28] R. Li, C. Cheng, F. Ren, J. Chen, Y. Fan, J. Ding, and H. Wanga, Appl. Phys. Lett. **92**, 141115 (2008).
[29] Z. Jacob and E. E. Narimanov, Appl. Phys. Lett. **93**, 221109 (2008).
[30] J. Elser and V. A. Podolskiy, Phys. Rev. Lett. **100**, 066402 (2008).
[31] A. Fiore, V. Berger, E. Rosencher, P. Bravetti, and J. Nagle, Nature (London) **391**, 463 (1998).
[32] A. Yariv and P. Yeh, *Optical Waves in Crystals* (Wiley, New York, 2003).
[33] D. M. Whittaker and I. S. Culshaw, Phys. Rev. B **60**, 2610 (1999).
[34] M. Liscidini, D. Gerace, L. C. Andreani, and J. E. Sipe, Phys. Rev. B **77**, 035324 (2008).
[35] *Handbook of Optical Constants of Solids II*, edited by E. D. Palik (Academic Press, Orlando, 1991).
[36] C. Soci, D. Comoretto, F. Marabelli, and D. Moses, Phys. Rev. B **75**, 075204 (2007).
[37] M. Galli, F. Marabelli, and D. Comoretto, Appl. Phys. Lett. **86**, 201119 (2005).
[38] A. Giannattasio and W. L. Barnes, Opt. Express **13**, 428 (2005).
[39] Since along the directions of maximum symmetry the surface plasmon is purely TM polarized, we choose to work with a TM-polarized incident field. On the other hand, the polarization is not preserved in all other directions on reflection, and so we plot the total reflectance as given by the sum of TE and TM intensities. If other procedures were adopted, the qualitative nature of the results would not change.
[40] M. D'yakonov, Sov. Phys. JETP **67**, 714 (1988).
[41] I. Abdulhalim, J. Opt. A, Pure Appl. Opt. **1**, 646 (1999).